Nonlinear waves and shocks in a rigid acoustical guide

Rasika Fernando[a] and Yann Druon
Airbus Operations S.A.S, Acoustics Department, Turbomachinery Acoustics, 31060 Toulouse, France

François Coulouvrat[b] and Régis Marchiano
Université Pierre et Marie Curie - Paris 6, Institut Jean Le Rond d'Alembert (UMR CNRS 7190), 4 place Jussieu, 75252 Paris cedex 05, France

(Received 17 June 2010; revised 7 October 2010; accepted 14 November 2010)

A model is developed for the propagation of finite amplitude acoustical waves and weak shocks in a straight duct of arbitrary cross section. It generalizes the linear modal solution, assuming mode amplitudes slowly vary along the guide axis under the influence of nonlinearities. Using orthogonality properties, the model finally reduces to a set of ordinary differential equations for each mode at each of the harmonics of the input frequency. The theory is then applied to a two-dimensional waveguide. Dispersion relations indicate that there can be two types of nonlinear interactions either called "resonant" or "non-resonant." Resonant interactions occur dominantly for modes propagating at a rather large angle with respect to the axis and involve mostly modes propagating with the same phase velocity. In this case, guided propagation is similar to nonlinear plane wave propagation, with the progressive steepening up to shock formation of the two waves that constitute the mode and reflect onto the guide walls. Non-resonant interactions can be observed as the input modes propagate at a small angle, in which case, nonlinear interactions involve many adjacent modes having close phase velocities. Grazing propagation can also lead to more complex phenomena such as wavefront curvature and irregular reflection. © *2011 Acoustical Society of America*.
[DOI: 10.1121/1.3531799]

PACS number(s): 43.25.Cb, 43.25.Jh, 43.28.Mw, 43.20.Mv [ROC] Pages: 604–615

I. INTRODUCTION

Nonlinear effects in acoustic waveguides are encountered in a wide range of applications. In musical acoustics, for instance, where they have received since recently a broad attention. The case of planar shock waves formed in trombones played at fortissimo levels, and which are responsible for their bright metallic sound, is studied experimentally by Hirschberg *et al.*[1] A simulation tool for shock formation and decay in pipes is then presented by Menguy and Gilbert[2] for short cylindrical tubes and by Gilbert *et al.*[3] for longer tubes of varying cross section. Their model is based on the resolution of the generalized Burgers' equation (Sugimoto[4]), which takes into account both the volume viscothermal effects and the losses due to the boundary layer.

In tubes closed at one end and with a piston at the other, planar shocks are also formed if the piston oscillates at a resonant frequency of the tube, thus generating harmonics which are all resonant frequencies. Chester[5] investigates an analytical solution for such resonant oscillations and describes the effects due to the viscothermal losses. Vanhille and Campos-Pozuelo[6,7] later describe one-dimensional and two-dimensional (2D) finite-difference models for these stationary plane waves, which also take into account viscothermal effects. It is to be noted that these studies focus on shocks propagating in a viscous fluid on the planar mode only.

Guided shock propagation is also encountered in the field of aeronautics. For instance, when the large turbo-engines of modern aircraft run at top speeds during take-off, the flow around the fan blade tips can become transonic. At the blades' leading edges, a series of shock waves is, thus, generated and propagates upstream following a helical path in the engine air intake. The sound thereby produced is referred to as *Buzz-saw Noise* or *Multiple Pure Tone noise* (Philpot[8]). This denomination is due to the richness of the resulting spectra which present large numbers of tones at the engine shaft rotation frequency harmonics. This problem is addressed by McAlpine and Fisher,[9] who present a one-dimensional model for the propagation of a sawtooth wavetrain in a hard-walled or lined cylindrical duct, in the presence of an incoming uniform flow. Their model is based on Burgers' equation which is solved along the propagation path in the frequency domain. The truncation error of this method requires additional numerical viscosity which is dependent on the square of the frequency. Furthermore, liner attenuation is also introduced *ad hoc* on the first-order radial mode, according to the hypothesis that the shocks are located at the blade tips only. This clever way of taking into account the influence of the duct in a one-dimensional propagation model finds its limitations when considering that higher order modes can also be excited when engines function at transonic regimes.

More generally, higher order mode propagation can lead to two types of nonlinear interactions: (i) dispersive interactions between modes propagating with different phase velocities, leading to non-resonant generation of harmonics and (ii) nondispersive interaction between modes propagating with equal phase velocities, leading to resonant generation of

[a]Current address: Onera, DSNA, BP 72, 29 Av. de la Division Leclerc, 92322 Chatillon Cedex, France.
[b]Author to whom correspondence should be addressed. Electronic mail: francois.coulouvrat@upmc.fr

 0001-4966/2011/129(2)/604/12/$30.00

harmonics and eventually shock formation (van Doren[10]). The former have been initially investigated by Keller and Millman[11] in the case of a circular waveguide containing air. The authors present a solution based on a power series expansion of the acoustic velocity potential, the acoustic pressure, and the propagation constant. The leading order term is the solution in the linear theory. A multiple scales expansion method is later used by Nayfeh and Tsai[12,13] for sound propagation in a lined duct, as the liner prevents resonant generation of harmonics.

The second type of interactions, the nondispersive interactions, which can occur during finite amplitude sound propagation in rectangular waveguides are investigated by Vaidya and Wang,[14] who describe the self-excitation phenomena of the harmonics, and Ginsberg,[15] who later presents theoretical results which include both types of interactions (Ginsberg and Miao[16]).

Quasi-linear theory predictions have first been compared to the experimental data by Hamilton and TenCate[17] in the case of nondispersive interactions, for a mode propagating near cutoff, and sum and difference frequency generation[18] in rectangular hard-walled waveguides. The authors make reference to the works by Naze Tjøtta and Tjøtta[19] who investigate the nonlinear interactions of two plane waves propagating in non-colinear directions in a loss-less fluid and adapt their conclusions to the interactions occurring between different modes, which lead to sum and difference frequency generation.

A more detailed review of the various studies concerning the nonlinear propagation of higher order modes is given by van Doren.[10]

The current article presents a general model to address the problem of guided and fully nonlinear wave propagation, up to shock formation and beyond. The main contribution of this model is that shocks are enabled to propagate both on planar and non-planar modes, by taking into account a large number of harmonics and modes. We first introduce the theoretical background of this model: it is based on a nonlinear wave equation over the acoustic velocity potential, or Kuznetsov equation,[20] written under its non-dissipative form. We then suggest an original quasi-modal solution to this equation, whose amplitudes vary following the axial direction under the influence of nonlinearities. In order to compute their evolution, we derive a system of ordinary differential equations over these amplitudes by using appropriate orthogonality relations, which is then simplified by assuming their slow variation, and finally truncated over a finite number of harmonics and modes.

To solve this system, an appropriate set of conditions at the origin of the duct, which depend on its geometry and on the input pressure waveform, is required. In the present study, we focus on a 2D geometry: a hard-walled duct of constant width and of semi-infinite length. To validate this model, the nonlinear propagation of a plane wave beyond shock formation is first investigated and the numerical results are compared to an analytical solution found in the literature (Hamilton and Blackstock[21]). The main concern of this study being the propagation of higher order modes, a single mode at different frequencies and a combination of modes are then used as inputs.

The physical solutions, which will be described, present oblique shock formation and reflections on the duct walls. These are the results of the two types of nonlinear interactions between the harmonics and the modes which have been mentioned above. Solutions in the case of a cylindrical hard-walled duct are presented in previous papers by the authors (Fernando *et al.*[22,23]), in which azimuthal shock formation is also investigated.

II. THEORETICAL MODEL

A. Notations for linear guided waves

We begin with a brief recall of the linear theory of guided waves in order to introduce useful notations for the nonlinear model. An inviscid and homogeneous fluid at rest is considered, with ambient sound speed c_0 and density ρ_0. The fluid fills a semi infinite and straight guide of axis $z \geq 0$ and of constant transverse section S of arbitrary shape (see Fig. 1). We denote by $\mathbf{r}_\perp = (r_1, r_2)$, the spatial coordinates in the plane transverse to the z-axis, by ∂S, the guide lateral walls, and by $\mathbf{n}$, the wall normal unit vector (outward pointing). The guide walls are assumed to be perfectly rigid. The acoustical field (either the pressure field p or the potential field ϕ) satisfies the linear wave equation,

$$\frac{\partial^2 \phi}{\partial t^2} - c_0^2 \nabla^2 \phi = 0, \tag{1}$$

and the rigid boundary condition,

$$\nabla \phi \cdot \mathbf{n} = 0 \quad (\mathbf{r}_\perp \in \partial S). \tag{2}$$

A guided wave is a solution of the above problem sought under the form

$$\phi_n(\mathbf{r}_\perp, z, t) = A_n \Psi_n(\mathbf{r}_\perp) \exp(ik_{z_n} z) \exp(-i\omega_0 t), \tag{3}$$

where A_n is the mode amplitude, ω_0 is the angular frequency, $k_0 = \omega_0 / c_0$ is the wavenumber, and k_{z_n} is the axial

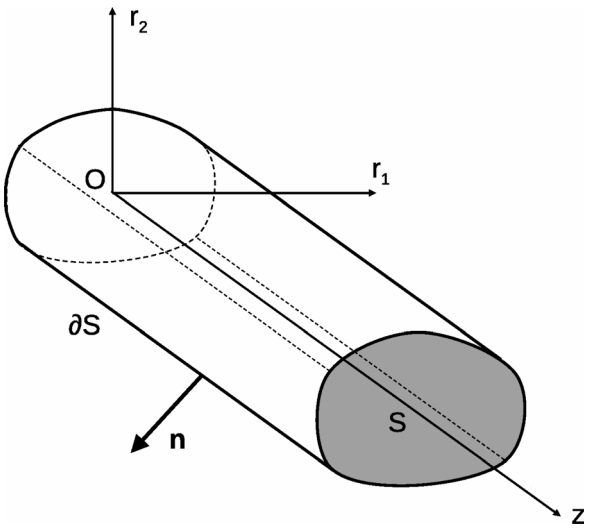

FIG. 1. Wave guide geometry.

wavenumber. The modal transverse distribution $\Psi_n(\mathbf{r}_\perp)$ satisfies the eigenvalue problem,

$$\nabla_\perp^2 \Psi_n(\mathbf{r}_\perp) = -\mathbf{k}_{\perp_n}^2 \Psi_n(\mathbf{r}_\perp), \tag{4}$$

associated to the boundary condition on the guide surface,

$$\nabla_\perp \Psi_n(\mathbf{r}_\perp) \cdot \mathbf{n} = 0 \quad (\mathbf{r}_\perp \in \partial S), \tag{5}$$

with $\nabla_\perp$ the transverse gradient. The square of the modulus of the transverse wavevector $\mathbf{k}_{\perp n}$ is one eigenvalue of the above problem. For rigid walls, eigenvalues are real. The index n belongs either to $\mathbb{N}$ or $\mathbb{N}^2$, depending on whether the geometry is at either two or three dimensions. The eigenvectors $\Psi_n(\mathbf{r}_\perp)$ constitute a basis and satisfy an orthogonality condition (Pierce[24] and Eversman[25]). They can be normalized so that

$$\frac{1}{S}\int\int \Psi_m(\mathbf{r}_\perp)\,\Psi_n(\mathbf{r}_\perp) dS = \delta_{mn}, \tag{6}$$

where δ_{mn} is the Kronecker delta ($\delta_{mn}=1$ if $m=n$ and $\delta_{mn}=0$ otherwise).

The axial and transverse wavenumbers are related through the dispersion relation so as to satisfy the wave equation

$$k_{z_n} = \sqrt{k_0^2 - k_{\perp_n}^2}. \tag{7}$$

Since the guide is assumed to be semi infinite, only forward propagating ($\Re e(k_{z_n}) \geq 0$) or evanescent ($\Im m(k_{z_n}) \geq 0$) modes are selected. Cut-on modes are those with a real axial wavenumber corresponding to propagating waves, while cut-off modes have an imaginary wavenumber associated to an exponential decay. Propagating modes have an axial phase velocity $c_n = \omega_0/\Re e(k_{z_n})$ which provides the dependence of the phase velocity with an angular frequency ω_0 and with the mode order n. At a given frequency, the field can, therefore, be written as a superposition of modes

$$\phi(\mathbf{r}_\perp, z, t) = \sum_n A_n \phi_n(\mathbf{r}_\perp, z, t). \tag{8}$$

B. The nonlinear model

Let us now investigate the nonlinear case. We remain in the regime of nonlinear acoustics, for which the amplitude of the wave is sufficiently large so that nonlinear effects have to be taken into account, but sufficiently small so that nonlinear terms other than quadratic ones can be neglected. This is equivalent to say that the *acoustical Mach number* $M_a = P_0/\rho_0 c_0^2$ with P_0 the maximum overpressure is much smaller than unity. For instance, a typical value for sound pressure levels (SPLs) inside aircraft engines is 170 dB, corresponding to a Mach number of 0.0456, indeed much less than unity. Hence, the low amplitude approximation is well satisfied and the acoustical field can be described with the well-known Kuznetsov equation[20]

$$\frac{\partial^2 \phi}{\partial t^2} - c_0^2 \nabla^2 \phi = -\frac{\partial}{\partial t}\left[(\nabla\phi)^2 + \frac{1}{c_0^2}\frac{B}{2A}\left(\frac{\partial \phi}{\partial t}\right)^2\right]. \tag{9}$$

The Kuznetsov equation is written in terms of the acoustical potential ϕ related to the velocity field $\mathbf{u}$ through the relation

$$\mathbf{u} = \nabla\phi \tag{10}$$

and to the acoustical pressure p through the relation

$$p = -\rho_0 \frac{\partial \phi}{\partial t} - \mathcal{L}. \tag{11}$$

In the above relation, compared to linear acoustics, an additional term appears involving the so-called Lagrangian density of energy:[26]

$$\mathcal{L} = \frac{1}{2}\rho_0 (\nabla\phi)^2 - \frac{\rho_0}{2c_0^2}\left(\frac{\partial \phi}{\partial t}\right)^2. \tag{12}$$

In Eq. (9), the coefficient B/A is the nonlinear parameter of the fluid describing the thermodynamic quadratic nonlinearity of the state equation relating pressure and density. Other nonlinear terms are *inertial* ones, coming from the nonlinearity of Euler equations. Note that, in Kuznetsov equation, no quasi plane wave approximation is performed, and the two types of nonlinear effects do not combine into a single one. This is different from simplified versions such as the Lighthill–Westervelt, Khokhlov–Zabolotskaya, or Burgers' equations.[21,27] Hence, the above Kuznetsov equation is quite general and is established only under the following two approximations: (i) the fluid is inviscid and (ii) the acoustical Mach number is sufficiently smaller so that cubic and higher order nonlinear terms are negligible. Note a generalized version of this equation, without this latter approximation is given by Söderholm.[28] Because of the smallness of M_a, linear terms on the left-hand side of Eq. (9) are of order M_a, while nonlinear ones on its right-hand side are 1 order of magnitude smaller (M_a^2).

A nonlinear guided wave is a solution of Eq. (9) associated to the boundary condition Eq. (2). We assume a time-periodic source in the initial plane $z=0$ with frequency $f_0 = \omega_0/2\pi$. That source can be either purely monochromatic or emit harmonics mf_0 ($m \in \mathbb{Z}$) (including the case of a shock wave at the source). Transverse pressure distribution can be general. In the linear case, as guided waves constitute a basis for a *rigid* guide, a general form of the solution that is periodic in time is given by

$$\phi(\mathbf{r}_\perp, z, t) = \sum_{m=-\infty}^{+\infty} \sum_n A_{m,n} \Psi_n(\mathbf{r}_\perp)\, \mathrm{e}^{ik_{m,n}z - im\omega_0 t}. \tag{13}$$

Here, notation $k_{m,n}$ is used for the axial wavenumber of the mode of order n at the frequency mf_0 satisfying the dispersion relation Eq. (7):

$$k_{m,n} = \sqrt{m^2 k_0^2 - k_{\perp_n}^2}. \tag{14}$$

In the nonlinear case, and even if the source is monochromatic, harmonics will be created (if they do not exist at the source) and will interact between one another as the

wave propagates along the guide. Hence, we are searching for a solution of the Kuznetsov equation under the general form

$$\phi(\mathbf{r}_\perp, z, t) = \sum_{m=-\infty}^{+\infty} \sum_n A_{m,n}(z)\Psi_n(\mathbf{r}_\perp)\, e^{ik_{m,n}z - im\omega_0 t}. \quad (15)$$

The only difference between the linear solution equations (13) and (15) is that the amplitudes of the modal decomposition now vary along the propagation axis, as modes will interact nonlinearly between one another as they propagate. Hence, the proposed model is called *quasi modal*. Obviously, because we use a modal decomposition in any transverse plane, the boundary condition, Eq. (2), is satisfied at any point. Also, because the signal is real, the coefficients satisfy the relation $A_{-m,n} = A^*_{m,n}$, where * designates the complex conjugate operator.

Now will be established the conditions to be satisfied by the amplitudes $A_{m,n}(z)$ so that the quasi-modal expansion Eq. (15) is a solution of Eq. (9). By direct substitution and after some tedious algebra, one gets

$$\begin{aligned} -c_0^2 \sum_{m=-\infty}^{+\infty} \sum_n \left[\frac{d^2A_{m,n}}{dz^2} + 2ik_{m,n}\frac{dA_{m,n}}{dz}\right]\Psi_n(\mathbf{r}_\perp)e^{ik_{m,n}z - im\omega_0 t} \\ = i\omega_0 \sum_{p=-\infty}^{+\infty} \sum_q \sum_{r=-\infty}^{+\infty} \sum_s (p+r) \\ \times A_{p,q}A_{r,s}\tilde{\Gamma}_{p,q,r,s}e^{i(k_{p,q}+k_{r,s})z}e^{-i(p+r)\omega_0 t}, \end{aligned} \quad (16)$$

where

$$\begin{aligned} \tilde{\Gamma}_{p,q,r,s}(\mathbf{r}_\perp, z) = \nabla_\perp\Psi_q(\mathbf{r}_\perp)\cdot\nabla_\perp\Psi_s(\mathbf{r}_\perp) \\ + \left[\left(\frac{d}{dz}\ln A_{p,q} + ik_{p,q}\right)\left(\frac{d}{dz}\ln A_{r,s} + ik_{r,s}\right) \right. \\ \left. - prk_0^2\frac{B}{2A}\right]\Psi_q(\mathbf{r}_\perp)\,\Psi_s(\mathbf{r}_\perp). \end{aligned} \quad (17)$$

The right-hand side of Eq. (16) describes the nonlinear interactions between various modes and frequencies, the nonlinear interaction of two fields of frequency pf_0 and rf_0 leading to a field of frequency $(p+r)f_0$ since nonlinearities are quadratic only. Hence, we can recover the mechanism of sum and difference (due to negative integers) frequency cascade. In the definition of Eq. (17), we can see three terms: the inertial nonlinearities associated to transverse variations of the field, the inertial nonlinearities associated to axial variations of the field, and the thermodynamic nonlinearities proportional to the nonlinear parameter B/A.

C. The weak amplitude assumption

Modal amplitudes vary under the effects of nonlinearities that are smaller than the linear effects. Hence, the left-hand-side of Eq. (16) is of order M_a, while the right-hand side is of order M_a^2. To overcome that inconsistency, one has to assume that amplitudes vary only slowly along the axis, e.g., that the axial derivatives describing the variations due to (locally small) nonlinear effects are of order M_a. As a consequence, in the left-hand side of Eq. (16), terms such as $dA_{m,n}/dz$ are indeed of the same order M_a^2 as right-hand side terms. This implies, however, that second order derivatives $d^2A_{m,n}/dz^2$ on the left-hand side are one-magnitude smaller (of order M_a^2) and first-order derivatives in the nonlinear right-hand side such as $d\ \ln\ A_{p,q}/dz$ are also 1 order of magnitude smaller than other nonlinear terms. As cubic nonlinearities are anyway neglected in the establishment of the Kuznetsov equation, it is fully consistent to neglect those various terms. This leads to a simplified first-order differential system

$$\begin{aligned} -2ic_0^2 \sum_{m=-\infty}^{+\infty} \sum_n k_{m,n}\frac{dA_{m,n}}{dz}\Psi_n(\mathbf{r}_\perp)e^{ik_{m,n}z - im\omega_0 t} \\ = i\omega_0 \sum_{p=-\infty}^{+\infty} \sum_q \sum_{r=-\infty}^{+\infty} \sum_s (p+r)A_{p,q}A_{r,s}\Gamma_{p,q,r,s} \\ \times e^{i(k_{p,q}+k_{r,s})z}e^{-i(p+r)\omega_0 t}, \end{aligned} \quad (18)$$

with

$$\begin{aligned} \Gamma_{p,q,r,s}(\mathbf{r}_\perp, z) = \nabla_\perp\Psi_q(\mathbf{r}_\perp)\cdot\nabla_\perp\Psi_s(\mathbf{r}_\perp) \\ - \left[k_{p,q}k_{r,s} + prk_0^2\frac{B}{2A}\right]\Psi_q(\mathbf{r}_\perp)\,\Psi_s(\mathbf{r}_\perp). \end{aligned} \quad (19)$$

In the definition of Γ in Eq. (19), we can see the same three terms as in $\tilde{\Gamma}$. The only difference is that in the inertial term associated to axial field variations, only the phase variations are taken into account, while amplitude variations are neglected. For propagating modes, we can introduce the angle $\theta_{m,n}$ made by the direction of propagation of the mode of order n at frequency mf_0 with the axis $k_{m,n} = mk_0\cos\theta_{m,n}$. Doing so, we can rewrite Γ in the following way

$$\begin{aligned} \Gamma_{p,q,r,s}(\mathbf{r}_\perp, z) = \nabla_\perp\Psi_q(\mathbf{r}_\perp)\cdot\nabla_\perp\Psi_s(\mathbf{r}_\perp) \\ - k_0^2 pr\beta(\theta_{m,n}, \theta_{r,s})\Psi_q(\mathbf{r}_\perp)\,\Psi_s(\mathbf{r}_\perp), \end{aligned} \quad (20)$$

where a nonlinear interaction coefficient between two modes comes out,

$$\beta(\theta_{m,n}, \theta_{r,s}) = \cos\theta_{m,n}\cos\theta_{r,s} + \frac{B}{2A}. \quad (21)$$

Such a coefficient has been introduced previously[18,19] to describe the nonlinear interactions of two plane waves that are not colinear. Once again, in that coefficient, two effects are involved: the thermodynamic effect (that is angle independent) and the inertial effect due to the convection of one wave by the other. In the plane wave case, one recovers the classical coefficient of non linearity $\beta = \beta(0,0) = 1 + B/2A$. Note here that, since the guided modes are not plane, the transverse variations are also taken into account in the definition of Γ. To further simplify the system in Eq. (18), the coefficients of the time Fourier series expansion are identified

$$\begin{aligned} -2ic_0^2 \sum_n k_{m,n}\frac{dA_{m,n}}{dz}\Psi_n(\mathbf{r}_\perp)e^{ik_{m,n}z} \\ = im\omega_0 \sum_q \sum_{r=-\infty}^{+\infty} \sum_s A_{m-r,q}A_{r,s}\Gamma_{m-r,q,r,s}e^{i(k_{m-r,q}+k_{r,s})z}. \end{aligned} \quad (22)$$

D. Projection

The final form of the system to be solved is obtained by projecting Eq. (22) on the basis of orthogonal modes. Multiplying Eq. (22) by Ψ_l, integrating over the guide's cross section S, and using the orthogonality relation, Eq. (6) yields

$$-k_{m,n}\frac{dA_{m,n}}{dz}e^{ik_{m,n}z}=\frac{m\omega_0}{2Sc_0^2}\sum_q\sum_{r=-\infty}^{+\infty}\sum_s A_{m-r,q}A_{r,s}\times\left[\iint\Gamma_{m-r,q,r,s}(\mathbf{r}_\perp)\Psi_n(\mathbf{r}_\perp)dS\right]\times e^{i(k_{m-r,q}+k_{r,s})z}. \quad (23)$$

Knowing the initial field in the plane $z=0$, the system of ordinary differential equations, Eq. (23), can be solved numerically, as will be shown in Sec. III. Note that the source term for the zero frequency $m=0$ is zero. Hence, all amplitudes $A_{0,n}(z)$ are constant and, due to the source assumptions, they will remain zero $A_{0,n}(z)=0$. The Kuznetsov equation does not allow to describe the phenomenon of streaming (acoustically induced steady flow), which is 1 order of magnitude smaller than the nonlinear terms considered here and requires a different theory.[29]

III. NUMERICAL METHOD FOR THE 2D CASE

A. Application of the model

A 2D rigid waveguide of width D and transverse variable x is now considered. Solutions of Eq. (4) are

$$\Psi_n(x)=\cos\left(\frac{n\pi}{D}x\right), \quad (24)$$

with $\mathbf{k}_{\perp n}=\alpha_n=n\pi/D$ and $n\in\mathbb{N}$. For a mode of order n at frequency mf_0, the cut-off frequency $f_{c,n}$, axial wavenumber $k_{m,n}$, phase velocity $c_{m,n}$, and propagation angle $\theta_{m,n}$ are given by

$$f_{c,n}=\frac{nc_0}{2D},\qquad k_{m,n}=mk_0\sqrt{1-\left(\frac{f_{c,n}}{mf_0}\right)^2},$$
$$c_{m,n}=\frac{c_0}{\sqrt{1-\left(\frac{f_{c,n}}{mf_0}\right)^2}},\qquad \tan\theta_{m,n}=\frac{nc_{m,n}}{2Dmf_0}. \quad (25)$$

At this stage, an important property has to be noted: for a given (input) mode (m,n), all modes of frequency $l\times m$ and of order $l\times n$ with $l\in\mathbb{N}$ any integer propagate with the *same* phase velocity $c_{m,n}$ and in the same direction $\theta_{m,n}$. Therefore, $c_{l\times m,l\times n}=c_{m,n}$ and $\theta_{l\times m,l\times n}=\theta_{m,n}$.

Given the simple expressions of the eigenmodes, coefficients of Eq. (23) can be computed in a closed form. After some tedious calculations, one gets the following system:

$$-k_{m,n}\frac{dA_{m,n}}{dz}e^{ik_{m,n}z}=\frac{m\omega_0}{4c_0^2}\sum_{r=-\infty}^{+\infty}\sum_{s=0}^{+\infty}[A_{m-r,n+s}A_{r,s}C_{m-r,n+s,r,s}\times e^{i(k_{m-r,n+s}+k_{r,s})z}-A_{m-r,n-s}A_{r,s}C_{m-r,n-s,r,s}\times e^{i(k_{m-r,n-s}+k_{r,s})z}], \quad (26)$$

where

$$C_{m-r,n\pm s,r,s}=\alpha_{n\pm s}\alpha_s\mp k_{m-r,n\pm s}k_{r,s}+k_0^2\frac{B}{2A}(m-r)r. \quad (27)$$

By recalling that $A_{-m,n}=A_{m,n}^*$, the right-hand side of the above system can be reduced to a summation on positive frequencies only. The total number of frequencies is then truncated to the first M harmonics ($m=1\rightarrow M$), and the total number of spatial modes is $N+1$ ($n=0\rightarrow N$).

B. Principles of the numerical method

The system of ordinary differential equations, Eq. (26), is solved, thanks to a classical fourth order Runge-Kutta algorithm with a fixed advancement step Δz. Evanescent modes introduce exponentially small or large terms that induce numerical instability after some propagation distance. Comparison of various simulations done with or without these modes shows no difference, as long as the simulations remain stable. Our own tests confirm those of van Doren.[10] Hence, it is believed that this behavior is purely numerical. That point of view is also supported by the fact that nonlinear energy transfers occur mostly between the modes having the similar phase velocity, as will be shown later on. The phase velocity of evanescent modes being undefined, we expect transfers between cut-on and cut-off modes to be small. Hence, in practice, for a given truncature up to order M in terms of frequency, all propagating modes for all frequencies between f_0 and Mf_0 are taken into account, which fixes the truncation $N(m)$ (which is then frequency dependent). Finally, nonlinear effects lead eventually to the formation of shock waves. Once shocks have formed, balance equations (from which the Kuznetsov equation is derived) are not sufficient to model shock waves. Here, given the fact that the time signal is expressed as a Fourier series through the model, we simply introduce a numerical viscosity that exponentially damps all components of the Fourier spectrum, with a coefficient proportional to the square of the frequency. Note that the approach is by no means original.[30,31] Physical thermoviscosity could theoretically be introduced into the model that way. However, in the targeted applications of fan noise in aircraft engine for the research project sustaining that work, the wave intensity is so high (acoustical Mach numbers are of the order 0.05) that the actual viscosity of air would imply keeping a very large number of frequencies. Moreover, at least for aeronautical applications, the dominant source of sound absorption is the wall attenuation due to liners, which is presently not included in this work. So, in order to capture the shocks, we have introduced a "higher than reality" numerical viscosity that is nevertheless sufficiently small to capture the physics of shock waves. Note that the present compromise is a very elementary example of the issue of "Large Eddy Simulation" problem in turbulence, where the discretization grid is much larger than the physical viscous scale. This implies to model in an adequate way the dynamics occurring at smaller scales not taken into account by the numerics.[32] This analogy is by no way surprising, as Burgers' equation, which is the basic equation for nonlinear acoustics, was originally proposed by Burgers as a model equation for turbulence.[33]

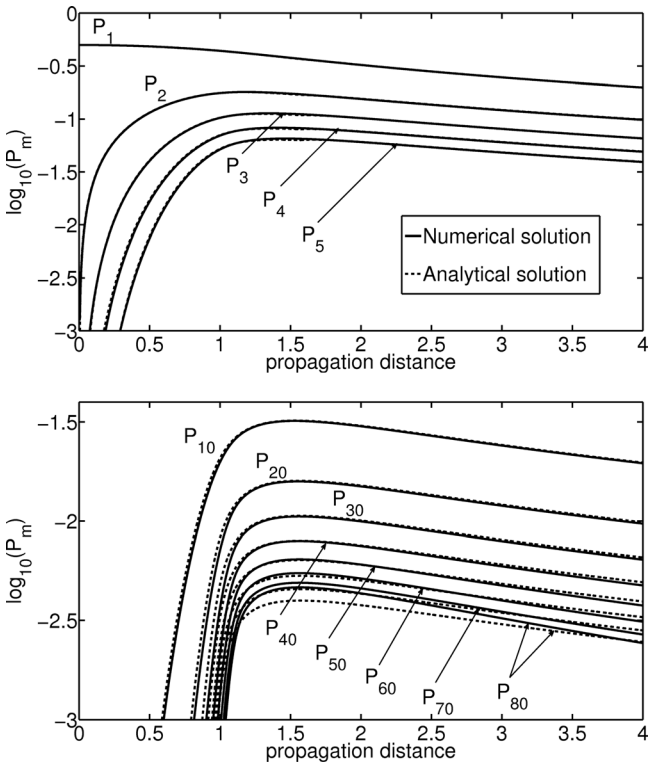

FIG. 2. Plane wave case. Numerical (solid line) and analytical (dashed line) pressure amplitude of harmonics 1 to 5 (top) and 10 to 80 (bottom).

C. Validation case

The numerical method is validated in the plane wave case $N=0$, when considering only modes of order 0. Then, it is easy to check that the model, Eq. (26), is equivalent to the Fourier series expansion of the inviscid Burgers' equation,[30] for which analytical solutions are well-known (Fubini solution before the shock[34] and Blackstock's extension beyond[35]). This case is used for a quantified validation of the method. The numerical solution is sought for an initially monochromatic plane wave. The number of retained harmonics is $M=100$, and the numerical viscosity is chosen inversely proportional to the number of harmonics.

The amplitudes of the harmonics along the propagation path are plotted and compared to the exact solution of the inviscid Burgers' equation in Fig. 2. These are the amplitudes $P_{m,n}$ of the acoustic pressure field, which are related to the acoustic velocity potential amplitudes $A_{m,n}$ by the linearized momentum conservation equation, written as follows in the spectral domain:

$$P_{m,n} = im\rho_0\omega_0 A_{m,n}. \tag{28}$$

The pressure amplitudes $P_{m,n}$ are computed locally, whereas the nonlinear effects are cumulative. In the quadratic order momentum conservation equation, Eq. (11), the latter are taken into account thanks to the Lagrangian density of energy defined in Eq. (12). This quantity being smaller by 1 order of magnitude than the linear term written in the right-hand side of Eq. (28), it is neglected in the computation of $P_{m,n}$.

In the present validation case, only the planar mode $n=0$ is taken into account. Therefore, the index n is neglected for the time being, and the amplitudes are written P_m. The results are presented in dimensionless variables, the pressure being scaled by its initial amplitude and the distance by the shock formation distance. For more clarity, the upper part of the figure presents in a logarithm scale the amplitude of the first five harmonics of the pressure field P_m ($m=1$ to 5) and the lower part from ten to ten $P_{m=10\times l}$ ($l=1$ to 8). One can observe a very good agreement, either before or after the shock formation distance (at $z=1$) between theoretical curves and numerical simulations. Nevertheless, the highest harmonics (see P_{80}) tend to be overestimated. This is due to the fact that the cascade of energy transfer from the fundamental to the higher harmonics is interrupted by the truncation. This induces an overestimation of about the latest 25% of the harmonics. However, because of the introduction of numerical viscosity, that overestimation does not impact the lower order harmonics. As a counterpart, the numerical viscosity tends to slightly underestimate the harmonics P_{10} to P_{40}, mostly before the shock formation, where the numerical viscosity already plays a role while the inviscid solution would conserve its energy.

IV. RESULTS

We are now considering the nonlinear propagation of guided non planar modes. We have investigated six different cases. In all cases, we have taken values representative for aircraft inlets in ambient air, with a guide of width $D=1$ m, an input pressure amplitude of $P_0=6500$ Pa, a sound speed $c_0=340$ m/s, a specific mass $\rho_0=1.2$ kg/m^3, and a nonlinear parameter $B/2A=0.2$. The modes of order $n=1$ and 2 have been studied, and for each case, two fundamental frequencies f_0 have been chosen, one close to the cut-off frequency for modes with a high propagation angle $\theta_{n,1}$ and one with a higher frequency and smaller angle. Values are reported in Table I. Table also provides the number of harmonics M and the highest number of modes N at the highest frequency Mf_0 retained in the numerical system. Let us recall that this last number is not user's chosen but is fixed by the fact that all propagating modes up to frequency Mf_0 are taken into account.

Figure 3 for configuration 1 and Fig. 4 for configuration 3 present the B-scan of the computed pressure field $p(x,z,t)$ at four given z propagation distances, equal, respectively, to 1, 2, 3, and 4 times the equivalent shock formation distance $L'=2L/\cos\theta_{n1}$. Quantity $L=\rho_0 c_0^3/\beta P_0\omega_0$ with $\beta=1+B/2A$ is the shock formation distance of a plane wave. The equivalent shock formation distance is an *estimation* of the shock formation distance for a guided mode, taking into account: (1) the inclination angle of the mode and (2) the fact

TABLE I. Computation configurations: n indicates the input mode order, f_0 the input fundamental frequency, $\theta_{n,1}$ the propagation angle of the input mode of order n at frequency f_0, M the frequency truncation, and N the mode truncation.

s	n	f_0 (Hz)	$\theta_{n,1}$ (deg)	M	N
1	1	171	84	50	50
2	1	240	45	50	70
3	1	1000	10	30	176
4	2	341	86	50	100
5	2	682	30	40	160
6	0 + 2 + 4	1000	0, 20, 43	30	100

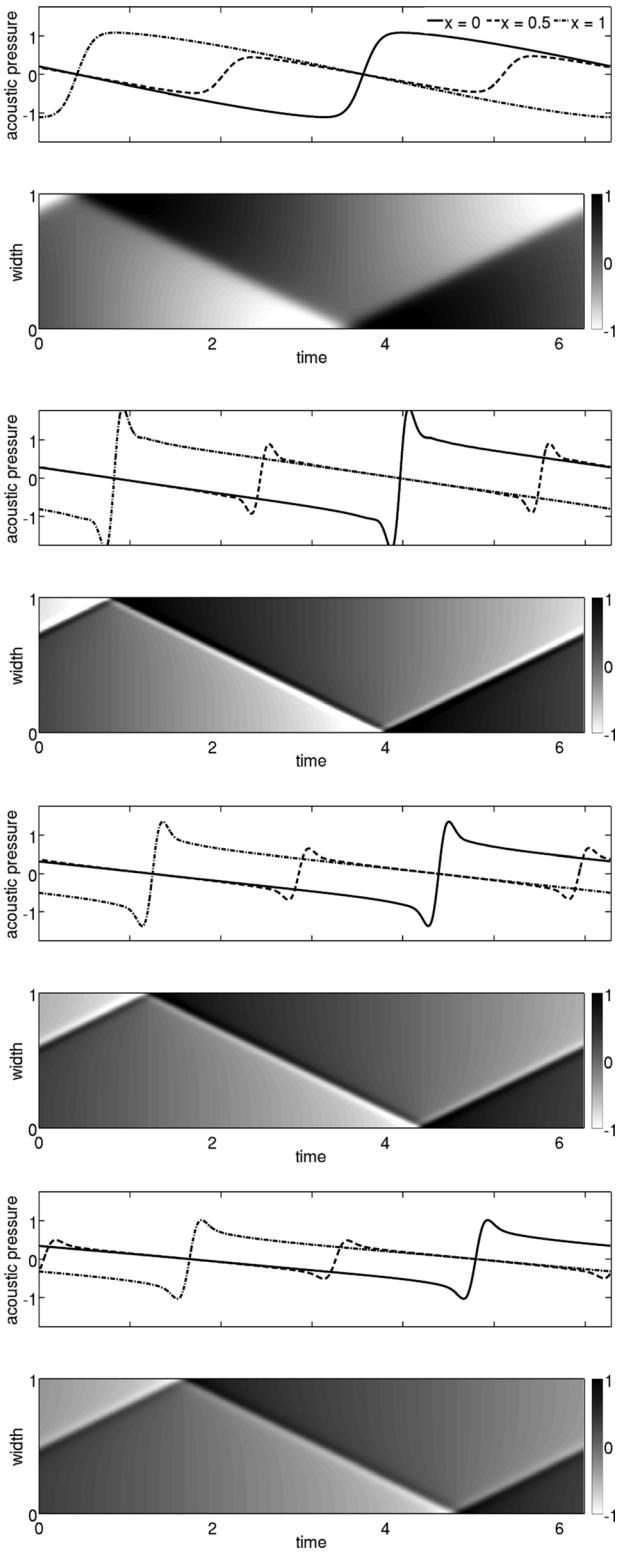

FIG. 3. Configuration 1. From top to bottom, axial distance z is, respectively, 1, 2, 3, and 4 times the equivalent shock formation distance. For each distance z, three pressure time waveforms are displayed on the top figure, respectively, $p(x = D/2, z, t)$ at the center of the guide, $p(x = 0, z, t)$ at its lower wall, and $p(x = D, z, t)$ at its upper wall. The lower figure displays the pressure B-scan $p(x, z, t)$.

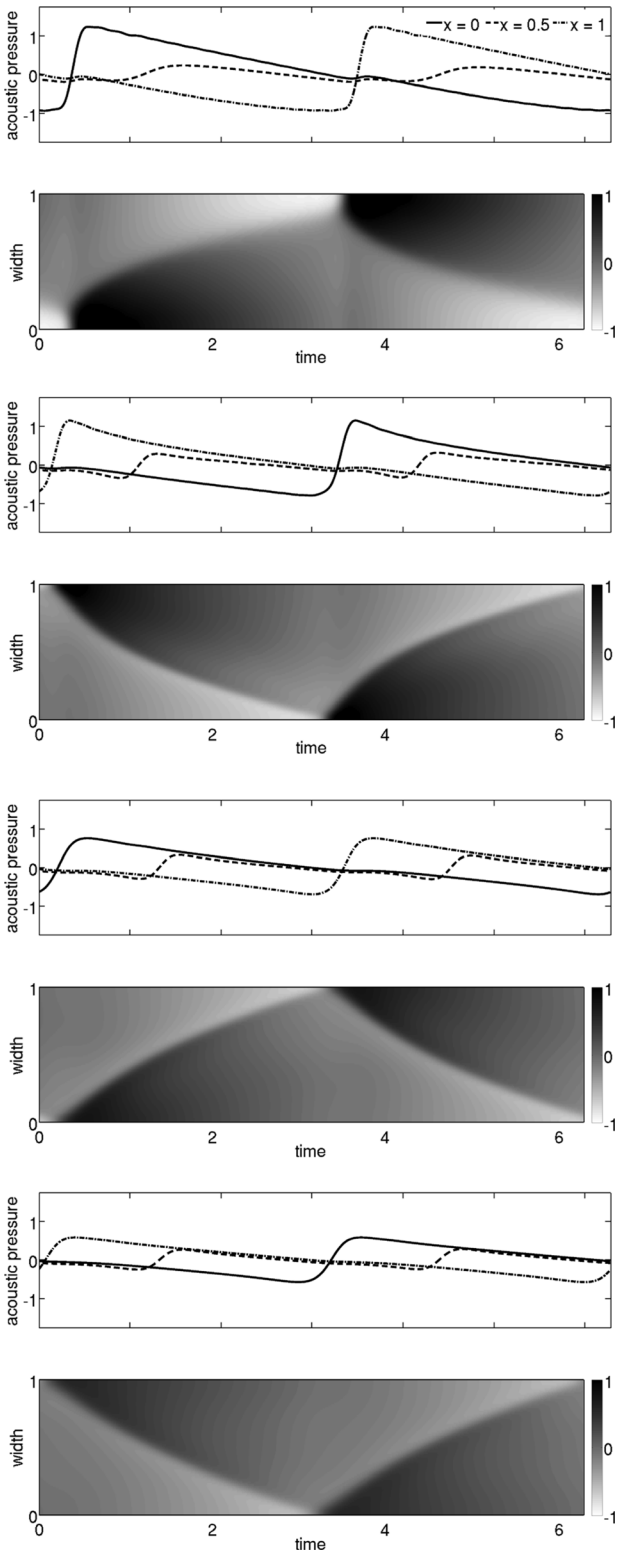

FIG. 4. Same as Fig. 3 for configuration 3.

that this one separates into *two* wavefronts that bounce on the guide walls. Except for grazing modes, we can expect these two wavelets to propagate more or less independently, hence the above definition of L'. The same figures also present the pressure time waveform at the center ($x = D/2$) and at the boundaries of the guide ($x = 0$ and D), at the same propagation distance. Figure 5 for configuration 1 and Fig. 6 for configuration 3 display the modal distribution of the field at the same distances $z = 1$, 2, 3, or $4L'$. The modal amplitude is relative to the amplitude of the input mode and is measured on a logarithmic scale for better visualization. By examining

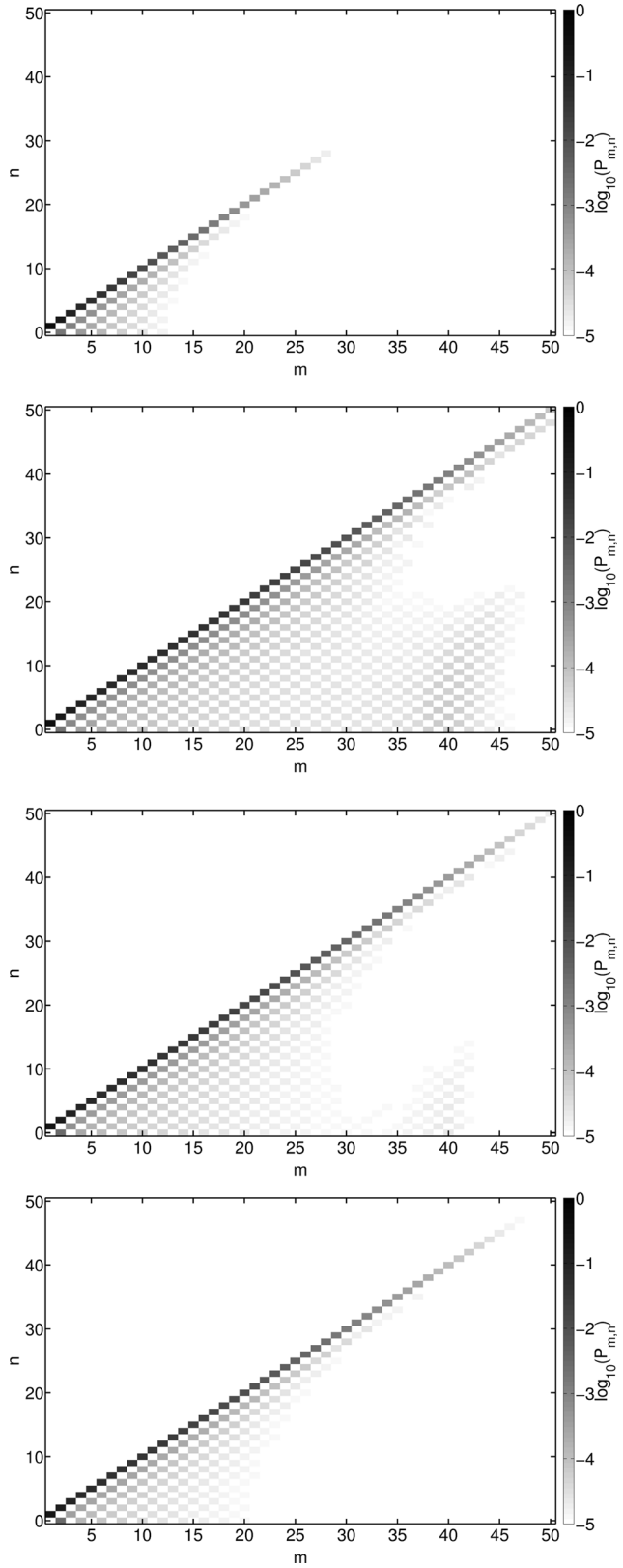

FIG. 5. Modal distribution of configuration 1 (logarithmic scale). From top to bottom, axial distance is, respectively, 1, 2, 3, and 4 times the equivalent shock formation distance.

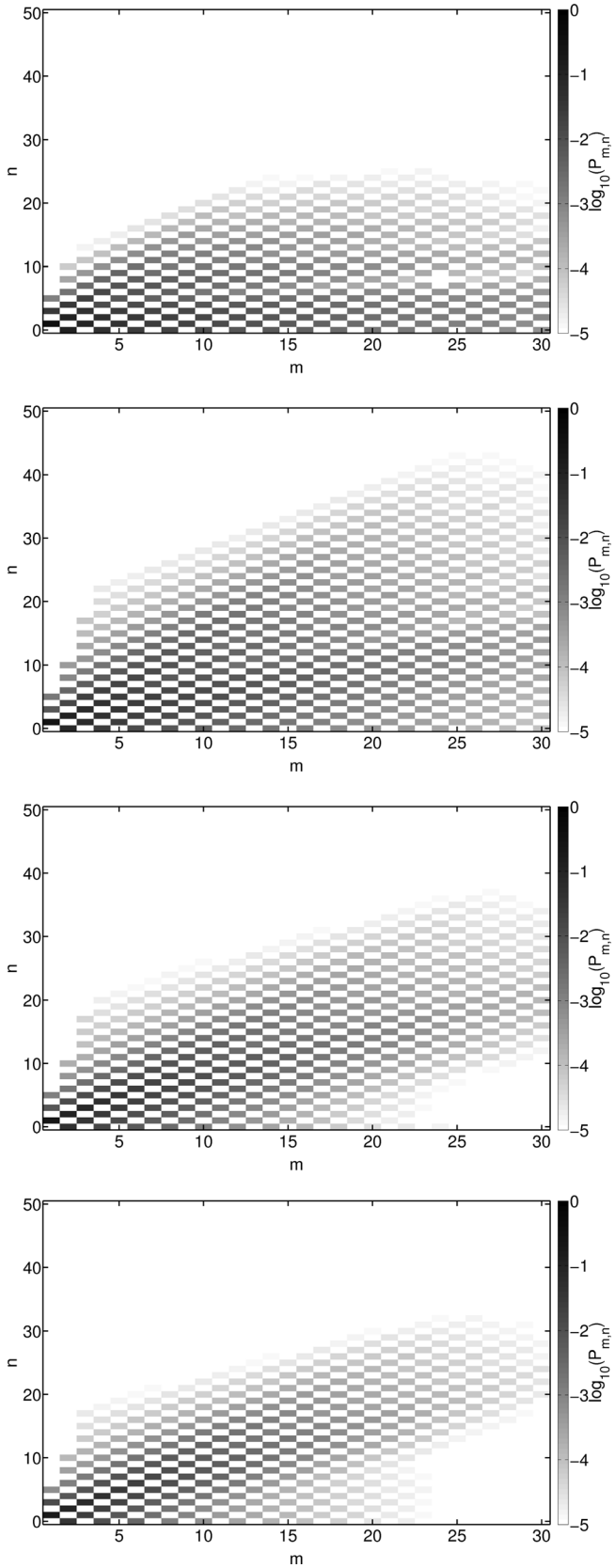

FIG. 6. Same as Fig. 5 for configuration 3.

these four figures, Figs. 3–6, one can make the following observations:

(1) In all cases, the formation of guided shocks is observed, with two shock fronts reflecting on the guide walls.

(2) For configuration 1, these shocks are almost perfectly straight.

(3) For configuration 1, the shock is not fully formed at the shortest propagation distance ($z = L'$).

(4) For configuration 3, the shocks are curved.
(5) For configuration 3, at the shortest propagation distance ($z = L'$), a triple point is visible with the two shock fronts merging not right at the guide wall but at some distance and being connected to the wall by a third shock (Mach shock).
(6) For configuration 1, starting from mode $n = 1$ at frequency $m = 1$, most of the energy transfers between modes involve only resonant modes of order $(l \times n)$ and of frequency $(l \times m)$ (dark diagonal on Fig. 5), e.g., modes propagating with the same phase velocity as the input mode. The interactions with other modes are not zero, but it is about 3 magnitude orders less intensive.
(6) For configuration 3, starting from mode $n = 1$ at frequency $m = 1$, nonlinear energy transfers between modes involve a much larger number of modes, with no preferred interactions with resonant modes Fig. 6.

V. DISCUSSION

Hence, there seems to be a fundamental difference between configurations 1 and 3. That difference is explained by examining the dispersion relations of the various modes in the two cases, Fig. 7. For configuration 1, the frequency is chosen so that the input mode is close to cut-off. Hence, the mode $n = 1$ is very inclined, and the mode phase velocity is very large, about nine times the sound speed. Only modes of order $l \times n$ and of frequency $l \times f_0$ have exactly the same phase velocity (dotted horizontal line on Fig. 7). These modes are called resonant modes because they all propagate with the same velocity, hence nonlinear interactions between them will not introduce any dispersion at all. They will, therefore, interact in a way similar to a plane wave, with harmonic cascade and shock formation. This explains why shocks in this case are almost perfectly straight. All other modes have a much slower phase velocity. Because of this phase velocity mismatch, energy transfers occur mostly between the resonant modes and very little with the other modes. Following the terminology of literature, such nonlinear interactions are called either resonant or non dispersive ones. On the contrary, for configuration 3, the frequency is chosen so that the input mode is only weakly inclined. Then, the phase velocity of mode $n = 1$ is close to the sound speed. Resonant modes of order $l \times n$ and of frequency $l \times f_0$ still have exactly the same phase velocity (dotted horizontal line on Fig. 7). However, a lot of neighboring modes have a phase velocity which differs only very slightly. Because phase velocity mismatches are now small, nonlinear interactions involve all these modes, as observed on the spectrum, Fig. 6. Following the terminology of literature, such nonlinear interactions are called either non-resonant or dispersive ones. Dispersion effects are visible in the fact that shocks are not as sharp as for the resonant case, and pressure waveforms are slightly asymmetrical (this is most visible for $z = 2L'$). Transfers of energy between various modes propagating at different angles induce a wavefront curvature that is very visible. Also visible, but only for $z = L'$ (top Bscan of Fig. 4) is the formation of a triple shock associated to the von Neumann type of irregular reflection. Indeed, the two main shock fronts (visible, respectively, as the white to gray and gray to black sharp transitions near the duct boundaries) do not match right on the duct surface as for regular reflection, but slightly away from it. A third shock, so-called Mach shock (white to black), perpendicular to the surface connects them to the surface and ensures the rigid boundary condition. It is known[36,37] that a step shock grazing over a rigid surface with an angle smaller than arcsin $\sqrt{2\beta P_0/\rho_0 c_0^2}$ will reflect in an irregular way, with a three-shock reflection pattern instead of the regular two-shock pattern observed for higher angles. Using the mode input value, the critical angle is 19.6°, larger than the mode angle equal here to 10°, in agreement with the observation of the von Neumann irregular reflection. Note, however, that the phenomenon does not persist all over the propagation (it is not visible anymore for $z = 2L'$ or further), as the shock amplitude decays through irreversible losses and the criteria is not satisfied any more after some propagation.[36] Configurations 2, 4, and 5 have also been investigated but figures are not reproduced here. As the angles are larger than the critical angle, only straight shocks are observed. For configurations 2 and 4, angles are large and, in a way very similar to configuration 1, resonant nonlinear interactions are very dominant compared to non-resonant ones. However, for configuration 5, the angle is not so large (30°). While resonant interactions are still most important, significant interactions with modes close to the diagonal of the resonant modes are observed. Hence, in this intermediate case, non-resonant interactions are not negligible anymore.

The final case, configuration 6, simulates an input field with multiple modes. We have selected a Gaussian transverse distribution

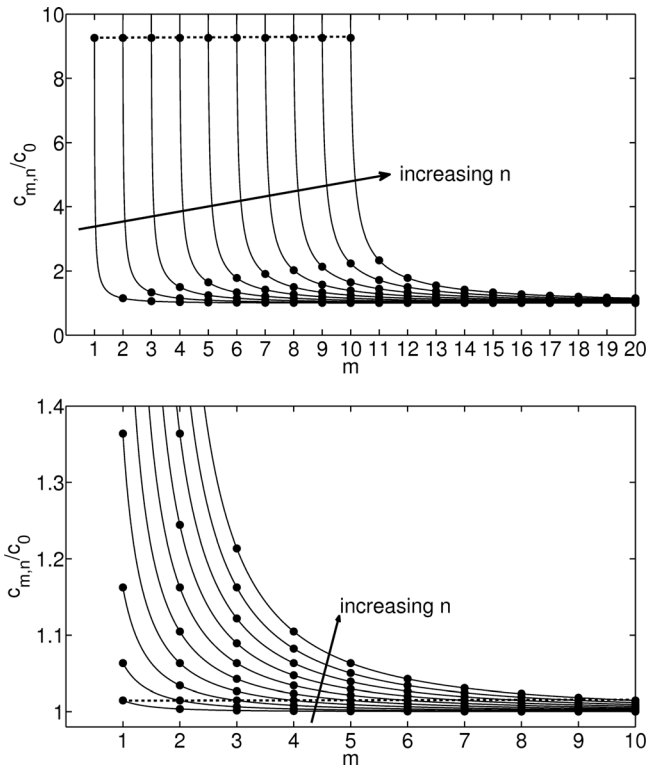

FIG. 7. Phase velocities of guided modes for harmonics mf_0 of the input frequency $f_0 = 171$ Hz (top) and $f_0 = 1000$ Hz (bottom). Arrows indicate increasing mode order n, from 1 to 10. Dotted lines link resonant modes.

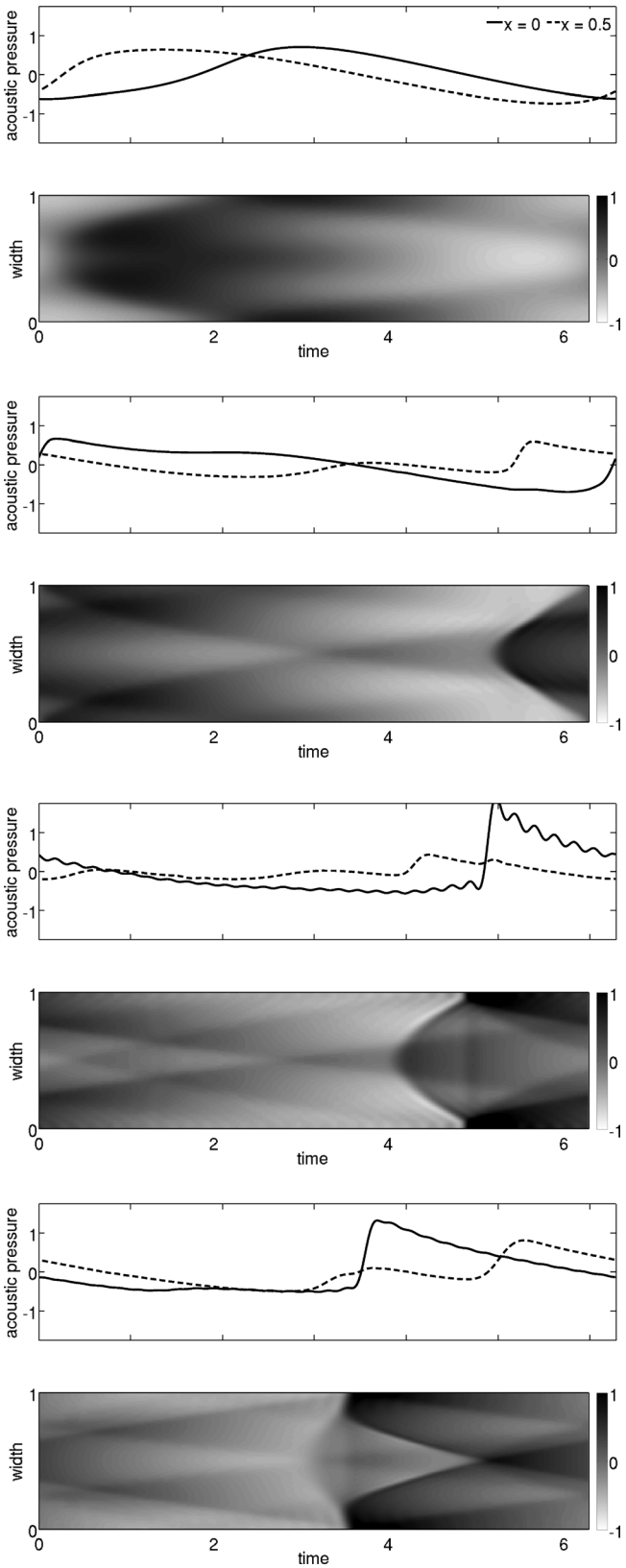

FIG. 8. Same as Fig. 3 for configuration 6.

$$p(x, z = 0) = \mathrm{e}^{-0.5((x/D-0.5)/0.1)^2 \mathrm{e}^{-i\omega_0 t}}, \tag{29}$$

at the source with frequency $f_0 = 1000$ Hz. Expanding the Gaussian into modes, only those of order $n = 0$, 2, 4 are propagating ones (odd modes do not contribute).

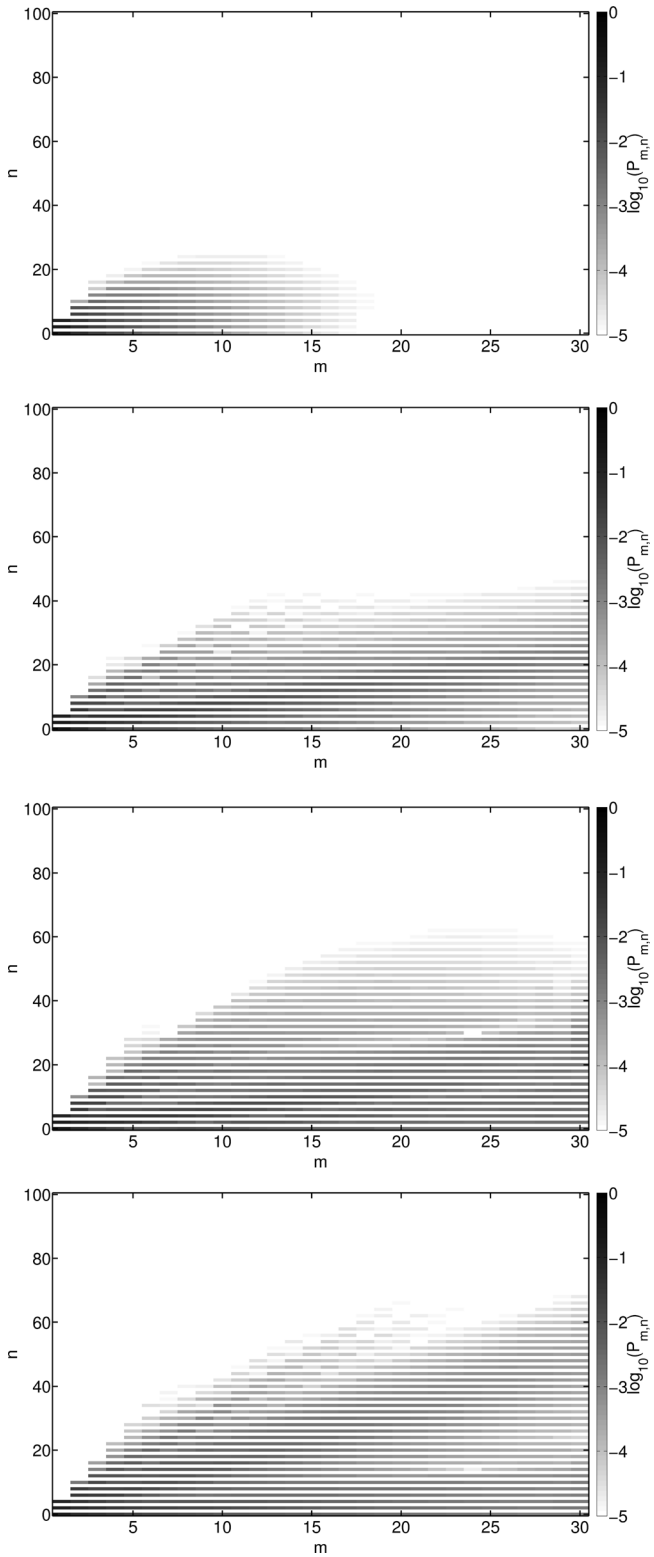

FIG. 9. Same as Fig. 5 for configuration 6.

As previously, Fig. 8 shows the B-scan and the time pressure waveforms of the computed pressure field $p(x, z, t)$ at four given propagation distances z equal, respectively, to 1, 2, 3, and 4 times the shock distance L. Here, because the source is composed of several modes, it is difficult to define an equivalent shock distance, so it is preferable to normalize the propagation distance with the shock formation distance associated to the plane mode $n = 0$. Figure 9 displays the

modal distribution of the field at the same distances. Because the input is even, only even modes of order $n=2q$ are generated. Since the frequency is high (1000 Hz), the input modes $n=0$ and 2 are relatively low inclined (their angles are, respectively, 0° and 20°) and their phase velocity are not very different from c_0 (respectively, 1 and 1.06 times c_0). Only the mode $n=4$ is more oblique (angle is 43° and phase velocity is 1.36 times c_0). Hence, dispersive and non dispersive interactions can take place simultaneously. This is visible on Fig. 9, where one can see the whole spectrum progressively filled as the wave propagates, but with more intensity along the three diagonals associated to each of the input mode. The complex input field leads to the formation of curved shock fronts. Because the mode is not plane, shock formation is delayed, somewhere between two and three times the plane shock distance. Some Gibbs oscillations appear at $z=3L$ at the guide wall where the pressure amplitude is maximum. Local amplification is observed near the guide walls at $z=3L$ and $4L$. This may be due once again to the nonlinear reflection effects, especially with the plane wave mode that is perfectly grazing. Note the wavefront curvature leads to the formation of a cusped shock caustic[38] between $z=3L$ and $4L$, with a typical swallow-tail wavefront visible in the center of the guide at $z=4L$.

VI. CONCLUSION

A model for guided nonlinear propagation of acoustic waves has been presented in this paper. The fundamental equation is Kuznetsov equation, written here under its inviscid form. A solution is sought after under a quasi-modal form. Mode amplitudes are assumed to vary slowly under the influence of the nonlinearities, and their evolution is computed by solving a system of first-order ordinary differential equations.

This model has then been applied to investigate the nonlinear propagation of acoustic waves in a hard-walled 2D duct of constant width. The numerical results for the propagation of a plane wave up to shock formation and beyond have been compared successfully (up to the 70th harmonic over a total of 100) to an analytical solution found in the literature.

Nonlinear propagation of higher order modes has also been studied. A single $n=1$ mode is used as input at different frequencies. For the lowest frequency, nondispersive interactions, between modes and harmonics propagating with equal phase velocity, are dominant and oblique and straight shock formation is observed. These shocks reflect in a regular fashion on the duct walls. For the highest frequency, the mode propagates close to the axis of the duct, and both dispersive and non dispersive interactions are observed, as energy shifts in a more homogeneous way toward all other propagating modes and harmonics of the truncation. The shocks which are formed in this case are curved, and irregular reflections are observed. The phenomena are quite similar when a Gaussian pressure distribution, resulting from a combination of modes, is used as input.

The application targeted by this model is finite amplitude sound propagation in turbo-engine air intakes. As said in the Introduction, the authors have presented in previous papers, the numerical results for the propagation of finite amplitude waves in a three-dimensional cylindrical hard-walled duct, filled with a fluid at rest (Fernando *et al.*[22,23]). To obtain better predictions, further enhancements have to be brought to this model, which still has to take into account (i) an incoming uniform flow and (ii) the inlet liner effects. Step (i) can be achieved by solving a "convected" Kuznetsov equation, following the method presented in the beginning of this paper, which uses the orthogonality properties of the eigenfunctions to derive the equations for the evolution of the amplitudes. The major difficulty in achieving step (ii) is that these eigenfunctions are not orthogonal in the case of lined walls, and projection of the equations is therefore prohibited. A way to get around this problem would be to use a *split-step* method which could solve alternately over small steps, nonlinear hard-walled propagation followed by linear lined propagation. Another and *a priori* more precise way to achieve this goal would consist in using the lined eigenmodes. Then, without performing the projection step of the present model, one would obtain a nonlinear matrix differential system instead of a system of ordinary differential equations and more advanced numerics would be necessary.

ACKNOWLEDGMENTS

R. F. has benefited from a CIFRE doctoral fellowship between Airbus France and Université Pierre et Marie Curie/Institut Jean Le Rond d'Alembert/CNRS (UMR 7190). The authors are grateful to Dr. Jean-Louis Thomas (CNRS) for the many helpful discussions. Professor Mark F. Hamilton (University of Texas at Austin) is thanked for forwarding us the Ph.D. dissertation of T. W. van Doren, which was a very useful source of information for preparing the present work.

[1]A. Hirschberg, J.Gilbert, R. Msallam, and A. P. J. Wijnands, "Shock waves in trombones," J. Acoust. Soc. Am. **99**, 1754–1758 (1996).
[2]L. Menguy and J. Gilbert, "Non-linear acoustic streaming accompanying a plane stationary wave in a guide," Acustica **86**, 249–259 (2000).
[3]J. Gilbert, L. Menguy, and M. Campbell, "A simulation tool for brassiness studies," J. Acoust. Soc. Am. **123**, 1854–1857 (2008).
[4]N. Sugimoto, "Burgers equation with a fractional derivative: Hereditary effects on non-linear acoustic waves," J. Fluid Mech. **225**, 631–653 (1991).
[5]W. Chester, "Resonant oscillations in closed tubes," J. Fluid Mech. **18**, 44–64 (1964).
[6]C. Vanhille and C. Campos-Pozuelo, "Numerical model for nonlinear standing waves and weak shocks in thermoviscous fluids," J. Acoust. Soc. Am. **109**, 2660–2667 (2001).
[7]C. Vanhille and C. Campos-Pozuelo, "Numerical simulation of two-dimensional nonlinear standing acoustic waves," J. Acoust. Soc. Am. **116**, 194–200 (2004).
[8]M. G. Philpot, "The buzz-saw noise generated by a high duty transonic compressor," ASME Paper, 70-GT-54 (1970).
[9]A. McAlpine and M. J. Fisher, "On the prediction of buzz-saw noise in aero-engine inlet ducts," J. Sound Vib. **248**, 123–149 (2001).
[10]T. W. van Doren, "Propagation of finite amplitude sound in multiple waveguide modes," Ph.D. dissertation, The University of Texas at Austin, 1993.
[11]J. B. Keller and M. H. Millman, "Finite-amplitude sound-wave propagation in a waveguide," J. Acoust. Soc. Am. **49**, 329–333 (1971).
[12]A. H. Nayfeh and M.-S. Tsai, "Nonlinear acoustic propagation in two-dimensional ducts," J. Acoust. Soc. Am. **55**, 1166–1172 (1974).
[13]A. H. Nayfeh and M.-S. Tsai, "Nonlinear wave propagation in acoustically lined circular ducts," J. Sound Vib. **36**, 77–89 (1974).

[14]P. G. Vaidya and K. S. Wang, "Non-linear propagation of complex sound fields in rectangular ducts, Part I: The self-excitation phenomenon," J. Sound Vib. **50**, 29–42 (1977).
[15]J. H. Ginsberg, "Finite amplitude two-dimensional waves in a rectangular duct induced by arbitrary periodic excitation," J. Acoust. Soc. Am. **49**, 1127–1133 (1979).
[16]J. H. Ginsberg and H. C. Miao, "Finite amplitude distortion and dispersion of a nonplanar mode in a waveguide," J. Acoust. Soc. Am. **80**, 911–920 (1986).
[17]M. F. Hamilton and J. A. TenCate, "Finite amplitude sound near cutoff in higher-order modes of a rectangular duct," J. Acoust. Soc. Am. **84**, 327–334 (1988).
[18]M. F. Hamilton and J. A. TenCate, "Sum and difference frequency generation due to noncollinear wave interaction in a rectangular duct," J. Acoust. Soc. Am. **81**, 1703–1711 (1987).
[19]J. Naze Tjøtta and S. Tjøtta, "Interaction of sound waves. Part I: Basic equations and plane waves," J. Acoust. Soc. Am. **82**, 1425–1428 (1987).
[20]V. P. Kuznetsov, "Equations of nonlinear acoustics," Sov. Phys. Acoust. **16**, 467–470 (1970).
[21]M. F. Hamilton and D. T. Blackstock, *Nonlinear Acoustics* (Academic Press, San Diego, 1998), Chap. 4, pp 113–114.
[22]R. Fernando, Y. Druon, R. Marchiano, and F. Coulouvrat, "A nonlinear computational method for the propagation of shock waves in aero-engine inlets—toward a new model for Buzz-saw Noise prediction," in *Proceedings of the 15th AIAA/CEAS Aeroacoustics Conference, AIAA Paper 2009–3238*, Miami, FL, 2009.
[23]R. Fernando, R. Marchiano, F. Coulouvrat, and Y. Druon, "Buzz-saw noise: Propagation of shock waves in aero-engine inlet ducts," in *Nonlinear Acoustics—Fundamentals and Applications (AIP Conference Proceedings 1022)*, edited by B. O. Enflo, C. M. Hedberg, and L. Kari (AIP, Melville, NY, 2008), pp. 99–102.
[24]A. D. Pierce, *Acoustics: An Introduction to its Physical Principles and Applications* (Acoustical Society of America, New York, 1989), Chap. 7, pp. 314–315.
[25]W. Eversman, *Aeroacoustics of Flight Vehicles—Theory and Practice*, Vol. 2, (Acoustical Society of America, New York, 1995), Chap. 13, pp. 101–163.
[26]S. I. Aanonsen, T. Barkve, J. Naze Tjøtta, and S. Tjøtta, "Distortion and harmonic generation in the nearfield of a finite amplitude sound beam," J. Acoust. Soc. Am. **75**, 749–768 (1984).
[27]F. Coulouvrat, "On the equations of nonlinear acoustics," J. Acoustique **5**, 321–359 (1992).
[28]L. H. Söderholm, "A higher order acoustic equation for the slightly viscous case," Acustica **87**, 29–33 (2001).
[29]L. Menguy and J. Gilbert, "Weakly nonlinear gas oscillations in air-filled tubes; solutions and experiments," Acustica **86**, 798–810 (2000).
[30]A. Korpel, "Frequency approach to nonlinear dispersive waves," J. Acoust. Soc. Am. **67**, 1954–1958 (1980).
[31]A. McAlpine and M. J. Fisher, "On the prediction of 'buzz-saw' noise in acoustically lined aero-engine inlet ducts," J. Sound Vib. **265**, 175–200 (2003).
[32]P. Sagaut, *Large Eddy Simulation for Incompressible Flows* (Springer, Berlin, 2005), Chap. 5, pp. 91–186.
[33]J. M. Burgers, "A mathematical model illustrating the theory of turbulence," Adv. Appl. Mech. **1**, 171–199 (1948).
[34]E. Fubini, "Anomalie nella propagazione di ande acustiche de grande ampiezza (Anomaly of the propagation of acoustic waves of finite amplitude"), Alta Freq. **4**, 530–581 (1935).
[35]D. T. Blackstock, "Connection between the Fay and Fubini solutions for plane sound waves of finite amplitude," J. Acoust. Soc. Am. **39**, 1019–1026 (1966).
[36]S. Baskar, F. Coulouvrat, and R. Marchiano, "Nonlinear reflection of grazing acoustic shock waves: Unsteady transition from von Neumann to Mach to Snell-Descartes reflections," J. Fluid Mech. **575**, 27–55 (2007).
[37]M. Brio and J. K. Hunter, "Mach reflection for the two-dimensional Burgers' equation," Physica D **60**, 194–207 (1992).
[38]R. Marchiano, F. Coulouvrat, and J.-L. Thomas, "Nonlinear focusing of acoustic shock waves at a caustic cusp," J. Acoust. Soc. Am. **117**, 566–577 (2005).